CHALMERS
UNIVERSITY OF TECHNOLOGY

The analytic and numerical form-finding of minimal surfaces and their application as shell structures

Proceedings of the IASS Annual Symposium 2020/21 and the 7th International Conference on Spatial Structures
Inspiring the Next Generation
23 – 27 August 2021, Guildford, UK
S.A. Behnejad, G.A.R. Parke and O.A. Samavati (eds.)

The analytic and numerical form-finding of minimal surfaces and their application as shell structures

Alexander SEHLSTÖM* and Chris J. K. WILLIAMS

* Department of Architecture and Civil Engineering
Chalmers University of Technology
412 58 Göteborg, Sweden
alexander.sehlstrom@chalmers.se

Abstract

One usually thinks of minimal surfaces as being used for fabric and cable net structures. However, they can also be used as the geometry for a shell structure, in which case the stresses under load will depart from a uniform tension, and may include both tensile and compressive stresses. Any minimal surface with principal curvature coordinates can be constructed analytically using the fact that it can be expressed by a single function of a complex variable. But the analytical approach is, in general, quite complicated. We show a quick and easy numerical approach that automatically produces a minimal surface and the principal curvature coordinates at the same time applicable to any minimal surface whose boundaries are either principal curvature or asymptotic directions, or a combination of the two. Straight lines and cable boundaries form asymptotic lines, which are oriented at 45° angle to the principal directions on a minimal surface, and a surface that is normal to a sphere has a principal curvature direction as its boundary. If the surface is materialised with members following asymptotic directions, any load acting over a small patch of the surface is transferred as a force couple acting along with the asymptotic members that bound the patch. The same happens in continuous surfaces, and if the small patch is taken to the limit, the point load is transferred as a moment along with asymptotic directions.

Keywords: cable net, shell, minimal surface, principal curvature, differential geometry, form finding.

1 Introduction

Frei Otto believed that the ideal shape for a cable net is a minimal or soap film surface with a uniform tension under prestress, and he often used an equal mesh for his cable nets. However, equal meshes can only approximate a minimal surface. But if the net of cables follows the principal curvature directions of the surface, it is possible to produce 'true' tensioned minimal surfaces, subject only to the limitation of the fineness of the grid. The same applies if the forces are reversed, resulting in a grid of compressed bars.

Minimal surfaces [7] have everywhere zero mean curvature or, in other words, the two principal curvatures at any point have equal magnitude but opposite signs. In this paper, we limit our attention to minimal surface with negative Gaussian curvature, meaning the principal curvatures must also be non-zero. This excludes planar surfaces, which are minimal surfaces with no curvature and therefor no distinct principal directions.

Finding principal curvature coordinates is also relevant for other surfaces which have negative Gaussian curvature. Such surfaces are known as hyperbolic surfaces and if the mean curvature is small, they can be considered approximately minimal, and include structures such as fan vaults and cooling towers.

Principal curvature directions [9] are orthogonal and conjugate directions, so tangents of constant coordinate curves in a principal coordinate system must also. The orthogonal requirement mean that the mixed component of the first fundamental form of the surface is zero and the conjugate requirement that the mixed component of the second fundamental form of the surface is zero. If these requirements are fulfilled, the coordinate system forms an isothermal grid, which is a grid of flat curvilinear squares on the surface.

Any minimal surface with principal curvature can be constructed analytically using the fact that it can be expressed by a single function of a complex variable. This is a special case of the Weierstrass–Enneper parameterization, which uses two functions, but one of them effectively only controls the pattern of coordinates on the surface. The details of the analytical construction are discussed in (Sehlström and Williams [12]) and involves mappings of the coordinate system between real and complex spaces. Figure 1 illustrates the relations between the images obtained using the maps for a simple minimal cable net structure. The mathematics of the analytical expressions is generally very complicated, but, as will be shown later, it is easy to numerically form find minimal surfaces with principal curvature coordinates.

Besides principal curvature directions, we are also interested in asymptotic directions. These are directions on a surface which have zero normal curvature. By drawing Mohr's circle of curvature (Nutbourne [8]) through the principal curvatures marked on the horizontal axis representing the normal curvature, the angle between the principal and asymptotic directions can be found by considering the intersection of the circle and the vertical axis. Figure 2 illustrates Mohr's circle of curvature for some families of surfaces, and we see that for a minimal surface with negative Gaussian curvature, the angle between the principal and asymptotic directions is always 45°.

2 Equilibrium of the net

If a fine grid cable net is constructed following principal curvature directions on a minimal surface with constant force density, the cable net will be in static equilibrium and we may use this fact to study the equilibrium in more detail (Sehlström and Williams [12]).

Let the position vector describing all points on the surface be $\mathbf{p} = \mathbf{p}(\theta^1, \theta^2)$ where θ^1 and θ^2 are used to denote the curvilinear coordinates, which is the same as the perhaps more common notation using u and v. The covariant base vectors $\mathbf{p}_{,1} = \partial\mathbf{p}/\partial\theta^1$ and $\mathbf{p}_{,2} = \partial\mathbf{p}/\partial\theta^2$ are tangential to the curves $\theta^2 = \text{constant}$ and $\theta^1 = \text{constant}$ respectively. Since we required the grid to follow principal curvature directions, the covariant base vectors are orthogonal, that is, $\mathbf{p}_{,1} \cdot \mathbf{p}_{,2} = 0$, and their length is equal to the corresponding element length.

The force density τ, which is equivalent to the uniform surface tension, is the element tension divided by the element length (Schek [11]), and the vector representing the force in an element in the net is simply the force density multiplied with the covariant base vector aligned with the element. Thus, the vector $\mathbf{T}_i$ representing the tension in the four members $i = 1, 2, 3, 4$ meeting at a node in the grid are

$$\begin{aligned} \mathbf{T}_1 &= -\tau\mathbf{p}_{,1}, & \mathbf{T}_2 &= \tau\left(\mathbf{p}_{,1} + \mathbf{p}_{,11}\delta\theta^1\right), \\ \mathbf{T}_3 &= -\tau\mathbf{p}_{,2}, & \mathbf{T}_4 &= \tau\left(\mathbf{p}_{,2} + \mathbf{p}_{,22}\delta\theta^2\right), \end{aligned} \tag{1}$$

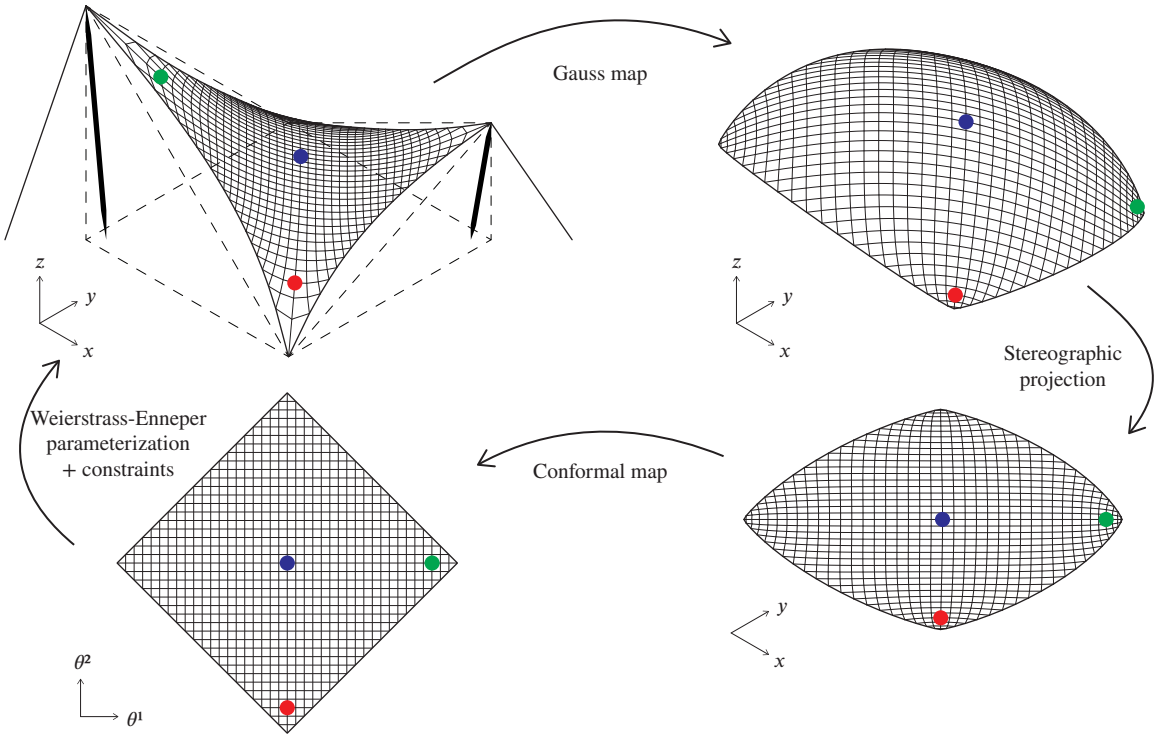

Figure 1: A minimal surface materialised as a cable net roof where the interior cables approximate the principal curvature directions and the boundary cables the asymptotic directions (top left) and its images after consecutively applying the Gauss map (top right), the stereographic projection (bottom right), and a conformal map $f(\zeta)$ which satisfy the Cauchy–Riemann equations (Spiegel [13, p. 63]) and $\zeta = \theta^1 + i\theta^2$ a complex variable (bottom left). The Weierstrass-Enneper parameterization enables mapping directly of a coordinate grid in complex space to the minimal surface in real three-dimensional space, but additional constraints are needed to obtain a principal curvature coordinate system. Mappings of three points are indicated using red, blue, and green dots in each of the images.

where $\delta\theta^1 = \delta\theta^2$ are the constant coordinate increments.

By combining the covariant base vectors $\mathbf{p}_{,1}$ and $\mathbf{p}_{,2}$ appropriately, other isothermal grids in static equilibrium on a minimal surface can be constructed. For example, the forces meeting at a node in a grid following the asymptotic directions are given by

$$\begin{aligned} \mathbf{T}_1 &= -\tau\left(\mathbf{p}_{,1} + \mathbf{p}_{,2}\right), & \mathbf{T}_2 &= \tau\left(\mathbf{p}_{,1} + \mathbf{p}_{,11}\delta\theta^1 + \mathbf{p}_{,2} + \mathbf{p}_{,22}\delta\theta^2\right), \\ \mathbf{T}_3 &= -\tau\left(\mathbf{p}_{,2} + \mathbf{p}_{,1} + \mathbf{p}_{,11}\delta\theta^1\right), & \mathbf{T}_4 &= \tau\left(\mathbf{p}_{,2} + \mathbf{p}_{,22}\delta\theta^2 + \mathbf{p}_{,1}\right). \end{aligned} \tag{2}$$

Regardless of the grid layout, the equilibrium of a ‘free’ cable boundary tells us that the geodesic curvature of the boundary must be constant and lie in the local tangent plane to the surface (Williams [15]). This means that the boundary must follow asymptotic directions. Furthermore, the force in each boundary must be constant along its length and thus the boundary will have varying force density, which is an exception from the requirement of a net with constant force density. Further more, a surface which is normal and fixed to a sphere has a principal curvature direction as its boundary on the sphere.

Figure 3 depicts two cable nets with the same boundary conditions and both approximate the same

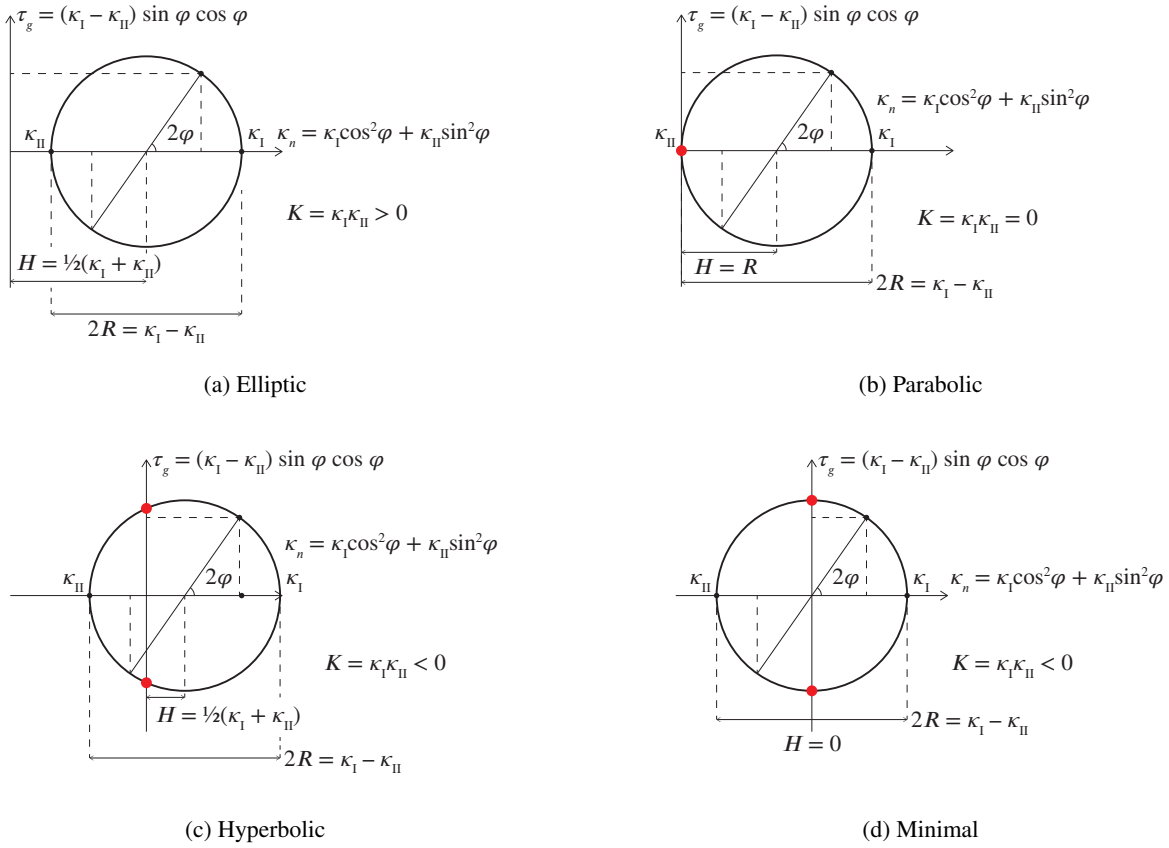

(a) Elliptic

(b) Parabolic

(c) Hyperbolic

(d) Minimal

Figure 2: Mohr's circle of curvature. Elliptic surfaces have no asymptotic directions, parabolic surfaces have exactly one asymptotic direction, and hyperbolic surfaces two asymptotic directions. Minimal surfaces with curvature are a type of hyperbolic surfaces where the angle between the principal and asymptotic directions always is 45°. A planar surface (not shown) has an infinite number of asymptotic directions, and any direction is an asymptotic direction.

underlying minimal surface. The net in fig. 3a follow principal curvature directions and the net in fig. 3b the asymptotic directions, and both have cable boundaries following the asymptotic directions. Their images under the Gauss map and the stenographic Gauss map are similar except for the orientation of the interior grid.

3 Continuous minimal surfaces with principal coordinates

If the minimal surface is materialised as a continuous surface, like Musmeci's bridge (fig. 4a), it can be analysed as a membrane shell with a capacity to carry membrane stress. Membrane stress is a combination of tensile, compressive, and shear stresses acting in a plane tangential to the surface, but of course, if a fabric is used, the capacity to carry compressive stresses is virtually zero since it will buckle.

The equilibrium of the surface is invariant, meaning the equilibrium equations are satisfied for any choice of coordinate system. But if the asymptotic directions are chosen, then the tensile or compressive stresses in the coordinate directions do not influence equilibrium in the normal direction. This means that we can establish the shear stress from equilibrium in the normal direction and then use that to study equilibrium

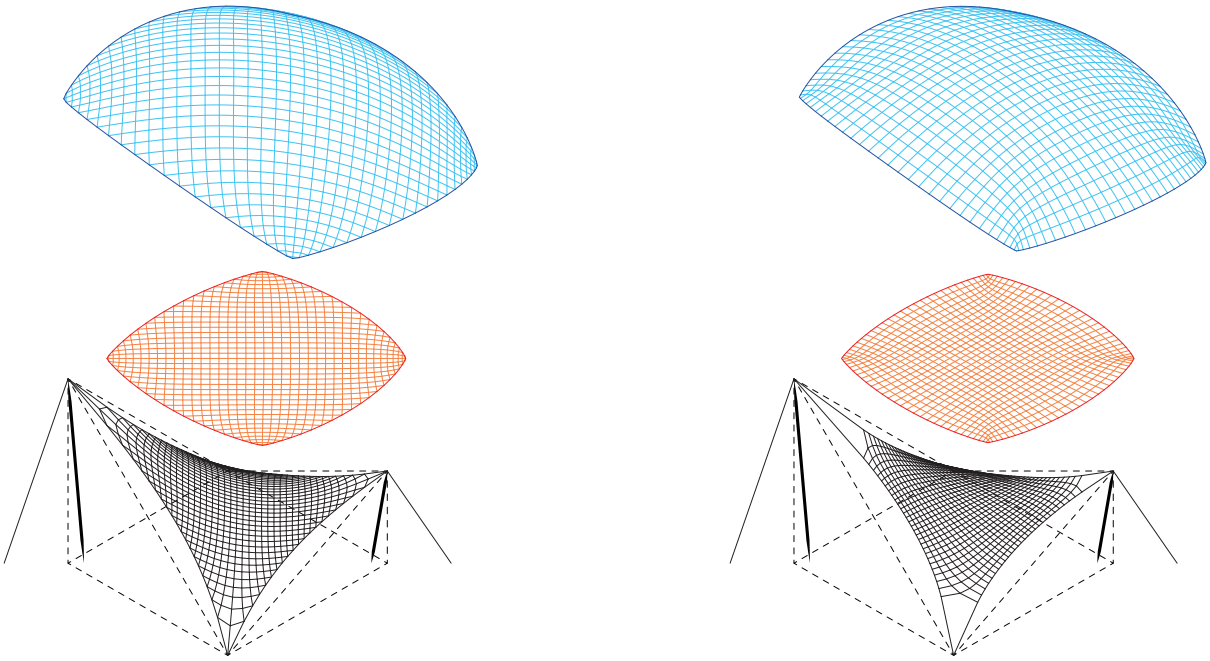

(a) Principal net.

(b) Asymptotic net.

Figure 3: Cable nets in static equilibrium (bottom, black) with their Gauss map (top, blue) and the south pole stereographic projections of the Gauss maps (middle, red).

(a) Image by unknown author, CC BY-SA 3.0, https://commons.wikimedia.org/w/index.php?curid=38867507.

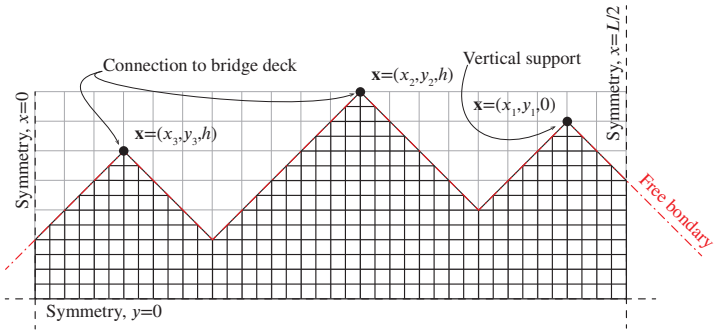

(b) Possible cutting pattern for a mesh that can be used for form finding of a minimal surface with principal curvature cables and similar boundary conditions as Musmeci's bridge.

Figure 4: The geometry of the substructure of the Musmeci's bridge across the Basento River was initially form found using a soap film model (Magrone et al. [6]).

tangential to the surface. This results in a hyperbolic system of equations in which we expect one end of each asymptotic line to reach a boundary, and the structure is statically determinate. If it does not reach any boundary, we have a mechanism, whereas if it does reach one boundary at each end, the structure is statically indeterminate.

We may solve the forces in the asymptotic members that bounds a small patch of the surface that is loaded with a force q by using an Airy stress function ϕ (Airy [1]) that is discontinuous (Williams and

McRobie [14]). The regions of ϕ corresponding to unloaded areas of the surface must be flat, but may slope, whereas the region corresponding to the loaded patch must be curved and the curvature is found solving Putcher's equation

$$z_{,11}\phi_{,22} - 2z_{,12}\phi_{,12} + z_{,22}\phi_{,11}, \tag{3}$$

where $z = z(\theta^1, \theta^2)$ is the shape of the surface, $\phi = \phi(\theta^1, \theta^2)$ the scalar valued stress function, and a comma denote partial differentiation such that, for example, $z_{,11} = \partial^2 z/(\partial\theta^1\partial\theta^1)$. For the discontinuous Airy stress function to satisfy equilibrium without any bending in the surface, neighbouring regions of ϕ must have the same value where they meet, resulting in 'folds' in the surface that should be understood as concentrated forces.

Figure 5 depicts a cantilevering hyperbolic paraboloid with asymptotic coordinates that is supported along the curved edge and loaded with a vertical force q acting over the small red patch which is a curvilinear square. Its projection onto the horizontal plane is an isosceles right triangle. The figure also depicts the discontinuous stress function ϕ from which we see that the force in the asymptotic members start at zero and linearly increases over the length that bounds the patch where after it is constant all the way to the support. Since the 'folds' along each pair of members have opposite direction, but equal angle, the force in the members are equal but of opposite sign.

If the size of the patch is taken smaller and smaller, the sloping regions between the asymptotic members tend to a vertical 'cliff,' which we at the limit may understand as a 'cut' in the surface corresponding to a bending moment acting about the surface normal whose magnitude is given by the difference in ϕ on either side of the cut (Williams and McRobie [14]).

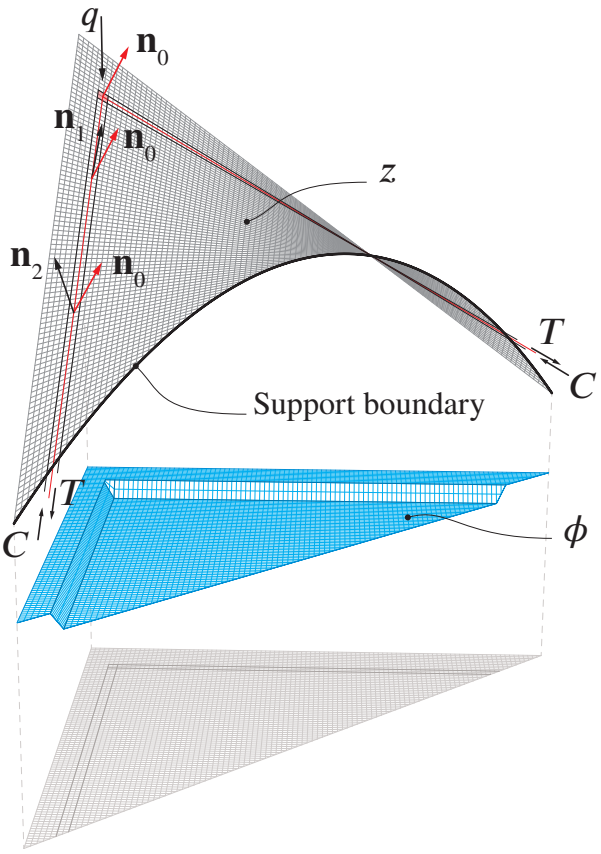

Figure 5: A patch load q acting on a hyperbolic paraboloid z and the corresponding discontinuous Airy stress function z. The patch load is transferred through the surface along asymptotic directions to the support as two force couples.

4 Numerical form finding

It is easy to numerically form find minimal surfaces with principal curvature coordinates using dynamic relaxation (Day [2]) and by representing the surfaces as a cable net following principal curvature directions. In dynamic relaxation, the nodal positions are consecutively updated until equilibrium is obtained. The updated position $\mathbf{x}_{a,i+1}$ of node a at time step i is given by

$$\mathbf{v}_{a,i+1} = \mu\mathbf{v}_{a,i} + \nu\Delta t\mathbf{a}_{a,i}, \tag{4}$$

$$\mathbf{x}_{a,i+1} = \mathbf{x}_{a,i} + \Delta t\mathbf{v}_{a,i+1}, \tag{5}$$

where $\mathbf{a}_{a,i}$ is the current acceleration of the node, $\mathbf{v}_{a,i}$ the current velocity, μ and ν numerical damping constants, and Δt the numerical time step.

In our case, we let $\Delta\mathbf{x}_{ab,i} = \mathbf{x}_{b,i} - \mathbf{x}_{a,i}$ be a vector along an element between nodes with position $\mathbf{x}_{a,i}$ and $\mathbf{x}_{b,i}$ respectively. Then the element length $\ell = |\Delta\mathbf{x}_{ab,i}|$ and the force in the element is $\tau\ell$. Thus, in analogy with eq. (1), the vector representing the tension the element ab subjects node a with become $\tau\Delta\mathbf{x}_{ab,i}$. From Newton's second law assuming a fictitious nodal mass $m = 1$ and setting the arbitrary but constant force density $\tau = 1$, the acceleration of node a at time step i become $\mathbf{a}_{a,i} = \sum_b \Delta\mathbf{x}_{ab,i}$ where the summation is done over all nodes b connected to node a.

Usually, the kinetic energy of the system or the norm of the nodal residual force is used as a convergence criterion for dynamic relaxation form finding. However, for minimal surfaces with principal curvature coordinates we know that the final grid should be isothermal. Therefor, as a convergence criteria, we may instead study the principal curvature curve lengths ratio and the asymptotic curve lengths ratio, both obtained by dividing the sum of the lengths in one direction divided by the sum of the lengths in the other direction. When both these ratios are 1, or close to 1, the solution has converged and we have an isothermal grid following principal curvature directions that is in static equilibrium and approximates a minimal surface.

4.1 Cutting pattern

The grid setup influences the form-finding result, and we may understand this setup by thinking of the initial grid as the image of the form-found grid as seen in complex space. Since the form-found grid will be isothermal, the image in the complex space is a regular grid. For a principal cable net, the regular grid in complex space align the horizontal and vertical axes in complex space (c.f. top left with the bottom left in fig. 1), whereas for an asymptotic net, the regular grid in complex space orients at 45° to the horizontal and vertical axes. Furthermore, since free edges must follow asymptotic directions, their image must be oriented at 45° to the horizontal and vertical axes in complex space. Thus, the initial grids used to form find the roofs in fig. 3 had the same boundary but different orientation of the interior elements; to get fig. 3a, the interior was aligned with the axes, whereas to get fig. 3b, the interior was aligned at 45° angle to the axes.

Figure 4b illustrates a cutting pattern and boundary conditions that can be used to form find a portion of a bridge similar to Musmeci's bridge connected to the rest via symmetry. The positions of the 'valleys' and 'ridges' on the free edge and their 'amplitudes' will affect the form finding and will most certainly require alterations to find a satisfying result. In addition to changing the grid setup, we may control the form-finding result by choosing different constant tensions for each of the four boundary segments (bound by lines of symmetry and/or black dots).

4.2 Kernel for parallel computation

Most dynamic relaxation implementations loops over a list of elements and computes the element contribution to the acceleration of the two nodes which the element spans between. The element axis and lengths are only computed once per element and time step, which is preferable since square roots are expensive to compute. Contributions to each node will be added to each node as many times as the node has connected elements; for a principal curvature cable net, the number of connected elements is four. Such a implementation works well if all element contributions are computed consecutively in a single thread, but not if they are computed in parallel threads since it would require costly thread concurrence locks to make sure only one thread updates each nodal acceleration at a time.

To make the implementation suitable for parallel computation, one can loop over the list of nodes instead and for each node sum up all the element contributions to that node in one single computation. Then

each nodal acceleration is only updated once, resolving the concurrency lock issue. This means that each element axis and length will be computed twice, but this drawback is ousted by the significant speed gains of computing in parallel.

The kernel outlined in algorithm 1 is suitable for parallel computing. It draws upon the concepts described in (Iványi [5]) with one list of current positions all thread can read from without interference and another list of updated positions that only the thread that computes the kernel for the node can write to.

We have implemented a solver in Java/Processing 3.5.4 where we can choose to execute the kernel in algorithm 1 consecutively in a single thread on the central processing unit (CPU) or in parallel using multiple threads on the graphics processing unit (GPU). The GPU computation relies on JavaCL which is a Java implementation of OpenCL. As can be seen in table 1, there is a significant speed improvement running the code in parallel. All ready with a simple integrated GPU, the code executes 15.8 times faster than on the CPU, and with a dedicated more powerful GPU, the code executes 60 times faster. The speed gain is of course dependent on the computer hardware, but similar improvements should be possible to see on most computers.

Algorithm 1: Kernel solving the updated nodal position $\mathbf{x}_{a,i+1}$ of node a in time-step i. The elements are part of a principal curvature net with constant force density τ in internal cables and with constant tension T in boundary cables. The algorithm assumes time-step $\Delta t = 1$. The numerical damping coefficients are typically set to $\mu = 0.995$ and $\nu = 0.2$.

Data: Current position $\mathbf{x}_{a,i}$ and current velocity $\mathbf{v}_a$
Result: Updated position $\mathbf{x}_{a,i+1}$ and updated velocity $\mathbf{v}_a$
for *each node b connected to node a* **do** `// may be done in parallel`
  $\mathbf{a}_a \leftarrow 0$; `// reset acceleration`
  $\Delta\mathbf{x}_{ab} \leftarrow \mathbf{x}_{b,i} - \mathbf{x}_{a,i}$; `// element axis`
  if *element ab is part of boundary cable* **then** `// add element contribution to acceleration`
    $\mathbf{a}_a \leftarrow \mathbf{a}_a + T/|\Delta\mathbf{x}_{ab}| \cdot \Delta\mathbf{x}_{ab}$; `// boundary cable`
  else
    $\mathbf{a}_a \leftarrow \mathbf{a}_a + \tau\Delta\mathbf{x}_{ab}$; `// interior cable`
  end
end
if *Node is constrained* **then**
  ; `// Apply boundary conditions, i.e. set components of the position vector` $\mathbf{x}_{a,i}$ `to prescribed values and set the corresponding components of the velocity vector` $\mathbf{v}_a$ `and acceleration vector` $\mathbf{a}_a$ `to zero.`
end
$\mathbf{v}_a \leftarrow \mu \cdot \mathbf{v}_a + \nu \cdot \mathbf{a}_a$; `// update velocity`
$\mathbf{x}_{a,i+1} \leftarrow \mathbf{x}_{a,i} + \mathbf{v}_a$; `// update position`

4.3 Example

Figure 6a shows a 'bridge' in the shape of a minimal surface with principal curvature coordinates form found using the presented kernel. Using a cutting pattern and boundary conditions indicated in fig. 6b, the form finding was done for a portion of the surface connected to the rest via symmetry. All nodes along the edge marked 'sphere constraint' are constrained to lay on the surface of a sphere normal to the surface and the outline of the sphere is shown in fig. 6c.

In addition to moving the nodes during the form finding, two boundaries are moved. Firstly, the bottom

Computation	**Processing unit**	**Processing specification**	**Time (ms)**	**Speed improvement**
Serial	CPU	Intel Xeon E3 1505M v5	543,852.06	1
Parallel	GPU (integrated)	Intel(R) HD Graphics P530	34,326.28	15.8
Parallel	GPU (dedicated)	NVIDIA Quadro M2000M	9,075.68	60.0
Serial	CPU	Intel Core i7 4790K	430,122.38	1.2
Parallel	GPU (dedicated)	GeForce RTX 2060 SUPER	4,414.45	123.2

Table 1: Computation time needed for different processing units to perform 100,000 dynamic-relaxation time-steps for a system consisting of 12,561 nodes.

of the sphere moves upwards a small distance linearly decreasing as the principal curve ratio approaches 1, and, secondly, the line boundary moves a small distance outwards in the y-direction linearly decreasing as the asymptotic length ratio approaches 1. Thus, the form finding is in this case a variation of Plateau's problem [3, 10, 4] where not only the minimal surface through a given boundary is found, but also the boundary itself.

As indicated in fig. 6c, some of the asymptotic members span between two funnels and are thus statically determinate and the rest span between a free edge and a funnel and are therefor statically determinate.

5 Conclusion

Minimal surfaces with principal curvature coordinates have been discussed, which can be used as geometry for tensioned cable nets and fabrics, as well as shell structures that may include both tensile and compressive stresses. Such surfaces can be found analytically, but it is, in general, quicker and easier to do the form-finding numerically. Principal coordinates on a minimal surface form a grid of curvilinear squares, and the asymptotic directions are simply the diagonals of the grid. If asymptotic members are used to materialise the surface, patch loads are transferred as a force couple acting along with the principal members that bound the patch, which at the limit becomes a moment. The same applies to continuous surfaces.

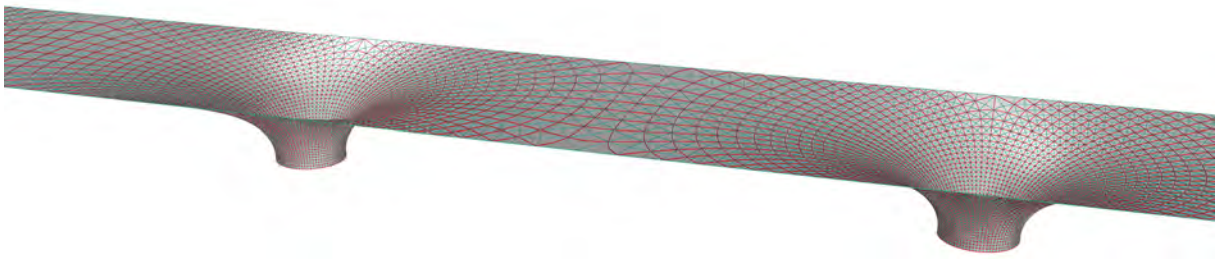

(a) Rendered bridge with red curves following principal curvature directions and blue asymptotic directions.

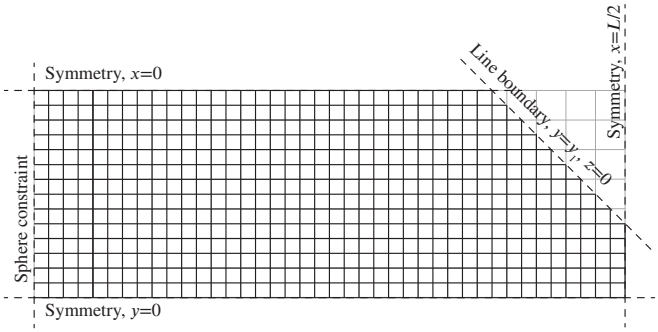

(b) Principle for the cutting pattern and the applied boundary conditions where L is the distance between the centre of the funnels.

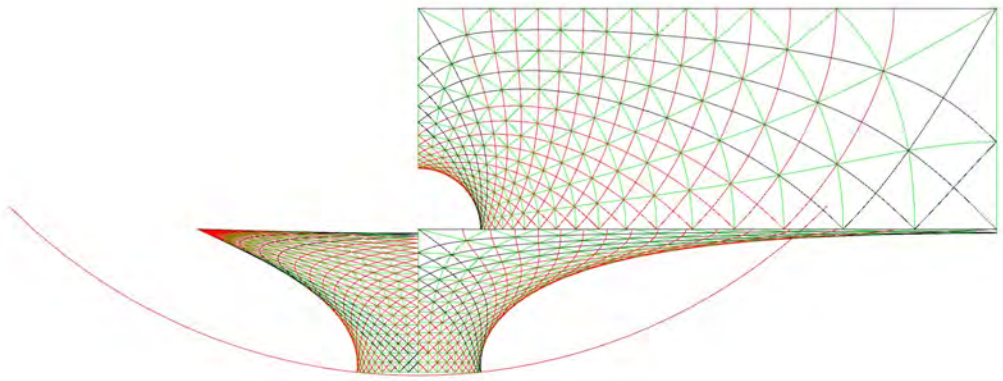

(c) Plan view and two elevations of form found surface with the boundary sphere is outlined. Green members follow principal curvature directions whereas black and red members follow asymptotic directions with black members being statically indeterminate and red statically determinate.

Figure 6: A 'bridge' in the shape of a minimal surface form found using coordinate curves following the principal directions.

References

[1] George Biddell Airy. "IV. On the strains in the interior of beams". In: *Philosophical Transactions of the Royal Society of London* 153 (Dec. 1863), pp. 49–79. DOI: 10.1098/rstl.1863.0004. URL: https://www.jstor.org/stable/108789.

[2] Alistair S. Day. "An introduction to dynamic relaxation". In: *The Engineer* 219 (1965), pp. 218–221.

[3] Jesse Douglas. "Solution of the problem of Plateau". In: *Transactions of the American Mathematical Society* 33.1 (1931), pp. 263–263. DOI: 10.2307/1989472.

[4] Jenny Harrison and Harrison Pugh. "Plateau's problem". In: *Open problems in mathematics*. Ed. by John Forbes Nash Jr. and Michael Th. Rassias. Springer International Publishing, 2016. Chap. 7, pp. 273–302. ISBN: 978-3-319-32160-8. DOI: 10.1007/978-3-319-32162-2_7.

[5] P. Iványi. "CUDA accelerated implementation of parallel dynamic relaxation". In: *Advances in Engineering Software* 125 (Nov. 2018), pp. 200–208. DOI: 10.1016/j.advengsoft.2018.02.008.

[6] P. Magrone et al. "Revisiting the form finding techniques of Sergio Musmeci: The bridge over the Basento River". In: *Structures and Architecture – Proceedings of the 3rd International Conference on Structures and Architecture, ICSA 2016*. Ed. by Paolo Cruz. Taylor & Francis Group, July 2016, pp. 543–550. DOI: 10.1201/b20891-75.

[7] "Minimal surface". In: *Encyclopedia of Mathematics*. URL: http://encyclopediaofmath.org/index.php?title=Minimal_surface&oldid=47844.

[8] A. W. Nutbourne. "A circle diagram for local differential geometry". In: *The Mathematics of surfaces: The proceedings of a conference organized by the Institute of Mathematics and its Applications and held at the University of Manchester, 17-19 September 1984*. Ed. by John Arthur Gregory. Oxford: Oxford University Press, 1986. ISBN: 0198536097.

[9] "Principal direction". In: *Encyclopedia of Mathematics*. URL: http://encyclopediaofmath.org/index.php?title=Principal_direction&oldid=42048.

[10] Tibor Radó. *On the problem of Plateau*. Ergebnisse der Mathematik und ihrer Grenzgebiete. 2. Folge. Berlin: Springer-Verlag, 1933. DOI: 10.1007/978-3-642-99118-9.

[11] Hans-Jörg Schek. "The force density method for form finding and computation of general networks". In: *Computer Methods in Applied Mechanics and Engineering* 3.1 (1974), pp. 115–134.

[12] Alexander Sehlström and Chris J. K. Williams. "Tensioned principle curvature cable nets on minimal surfaces". In: *Proceedings of the Advances in Architectural Geometry conference 2020*. Ed. by Olivier Baverel et al. Presses des Ponts, 2021, pp. 86–109.

[13] Murray R. Spiegel. *Schaum's outline of theory and problems of complex variables with an introduction to conformal mapping and its application*. SI (matric). Schaum's outline series. McGraw-Hill Book Company, 1974.

[14] Chris Williams and Allan McRobie. "Graphic statics using discontinuous Airy stress functions". In: *International Journal of Space Structures* 31.2-4 (June 2016), pp. 121–134. DOI: 10.1177/0266351116660794.

[15] Chris J. K. Williams. "Patterns on a surface: the reconciliation of the circle and the square". In: *Nexus Network Journal* 13.2 (2011), pp. 281–295. DOI: 10.1007/s00004-011-0068-2.